Benefits of Multi-Static on HF Radar Networks

Chad Whelan, Max Hubbard
CODAR Ocean Sensors, Ltd.
Mountain View, CA, USA
chad@codar.com

***Abstract*—Multi-static surface current vector data was processed for two different HF Radar networks, one measuring currents off the East Coast of the U.S. and the other measuring currents in the Malta Channel. Some effects of adding multi-static data are shown, including decreases in 2-D total vector uncertainties, increase in percent coverage within the network grid and increases in HF radar coverage area.**

Keywords—HF Radar; Multi-static;Bi-static; Surface Currents

I. Introduction

With large regional and national scale operational High Frequency Radar (HFR) networks having been implemented in the U.S. [1] and around the world [2], the need has increased for maximizing the coverage of a limited number of systems, optimizing quality control of the near real-time data products and providing data redundancy. Bi-static HF Radar measurement of sea echo has been studied since the early 1970's [3][4] and developed and evaluated for use in operational coastal monitoring networks [5][9][10] since then. Adding multi-static capability, in which individual HF radars can receive bi-static sea echo from multiple transmitters on the same frequency, can help with some or all three of these issues by increasing the number and density of surface current measurements in an HFR network. Multi-static processing has been shown to be able to provide quality data [7] and here it is now shown to deliver tangible benefits to operational networks. Two case studies of the effects of adding multi-static data outputs to existing SeaSonde HFR networks are shown below.

II. North Carolina & Virginia Network

A. Network Description

The four SeaSonde stations used in this study are part of the Mid-Atlantic Regional Association for Coastal Ocean Observing System (MARACOOS) network and located at Cedar Island, VA (CEDR), Little Island State Park, VA (LISL), the Army Corps of Engineers Field Research Facility in Duck, NC (DUCK), and Cape Hatteras, NC (HATY) as shown in Figure 1. All four stations were Long Range SeaSondes that operate in the 4-6 MHz band. CEDR, LISL and HATY sites were configured as standard Long Range sites with a single, omnidirectional transmit antenna. These sites typically achieve 180 – 200 km daytime range with reduced ranges in the evening of ~160 km due to evening increases in background RF noise via skywave propagation. DUCK was configured using a directional twin-transmit antenna, dual transmitter configuration for increased ranges of 225-240 km during the daytime and 180 – 200 km during the evening. In addition to the four SeaSondes, a transmit-only station was installed on Jennette's Pier in Nags Head, NC (JEAN). For this study, all four SeaSondes were tuned to the same center frequency of 4.537183 MHz and sweep bandwidth of 25.73 kHz. All systems operated continuously without mutual interference by employing frequency sharing with GPS-enabled time modulation multiplexing [6], also known as SHARE®.

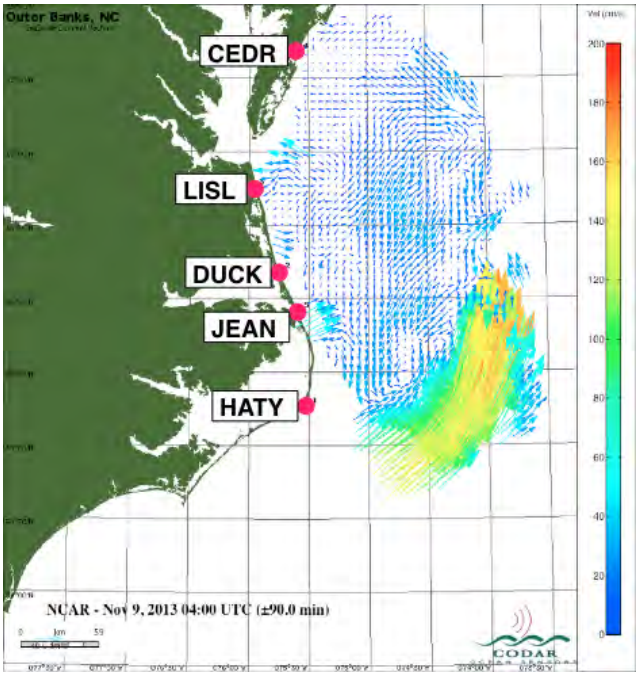

Fig. 1. Map of SeaSonde sites in the NC & VA network

B. Multi-Static Setup

With all systems operating with the precise timing that SHARE provides, the four SeaSonde stations and the bi-static transmit source, JEAN, were configured with precise timing to allow processing of a number of bi-static data sets that produce 1-D surface current vectors on an elliptical grid (aka ellipticals) [5]. The sweep offset timings of the systems were set to collect multi-static data as follows:

- LISL was configured to receive bi-static sea echo from both DUCK and JEAN transmitters. This resulted in two elliptical vector sets, LUCK and LEAN.
- DUCK was configured to receive bi-static sea echo from JEAN, resulting in the elliptical vector data set DEAN.

• CEDR and HATY shared the same frequency as the others but did not have timings set to receive bi-static sea echo or provide a transmit source to other stations.

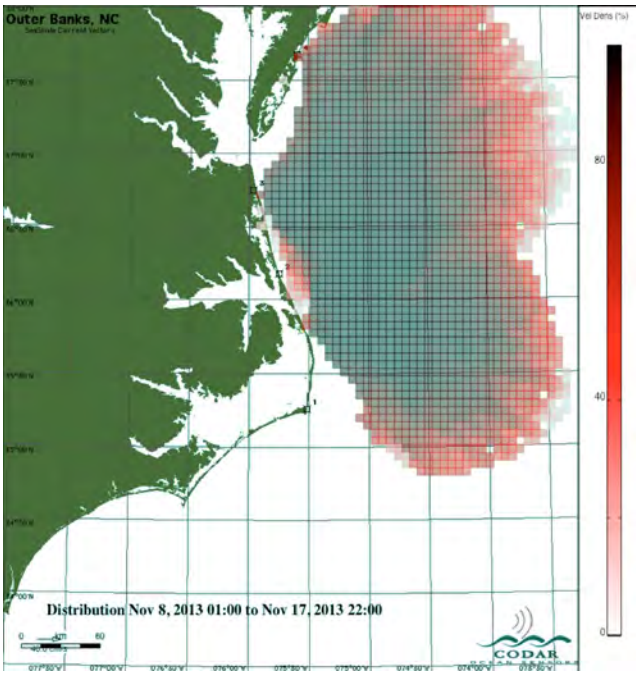

Fig. 2. Percent temporal 2-D coverage of total vectors when processing with mono-static radial vectors only

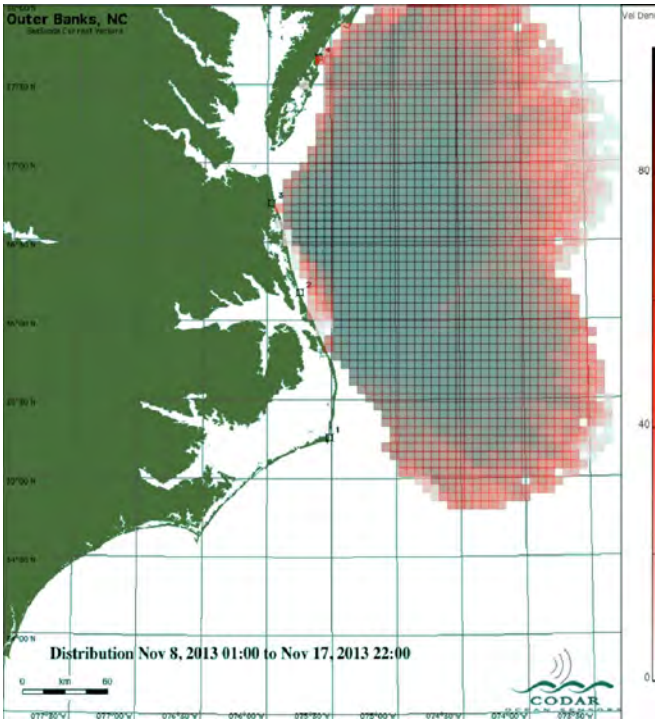

Fig. 3. Percent temporal coverage of 2-D total vectors processed with radial and elliptical vectors

Total (2-D) surface current vectors were first processed by combining 1-D radial vectors from the four SeaSondes only: CEDR, LISL, DUCK and HATY. Then they were processed by combining both radial and elliptical sources: CEDR, LISL, DUCK, HATY, LUCK, LEAN, and DEAN.

C. Percent Coverage Increased

Vector percent coverage plots for total vectors processed with and without elliptical vector sets are shown in Figures 2 & 3, respectively. The overall coverage area did not increase, which would be expected with a purely linear radar network, but darker shading in the coverage plot that includes elliptical vector data indicates that the internal grid points contained vectors a higher percent of the time. Approximately 30% of grid points saw increases in percent coverage. This appears to be consistent with the results found in [11].

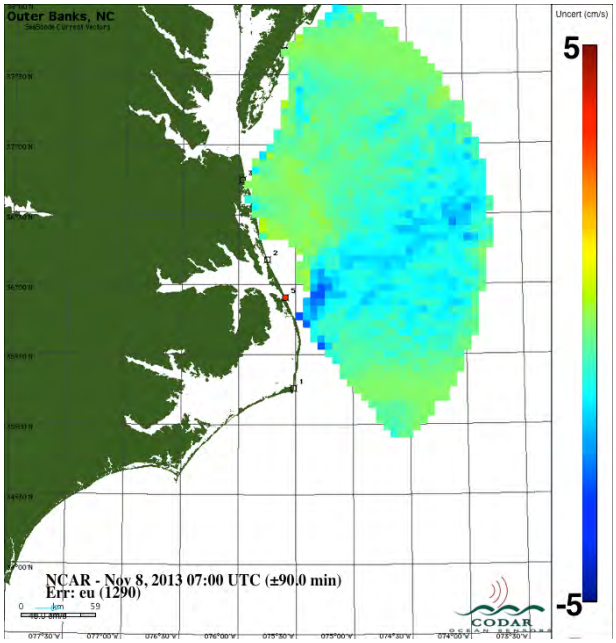

Fig. 4. Map of mean difference in U uncertainties (cm/s) by adding elliptical vectors

D. 2-D Vector Uncertainties

In addition to increasing temporal coverage for map grid points, inclusion of elliptical vectors should also improve quality of the vectors processed with radials only. In the process of combining radial and elliptical vector data into the gridded total vector data, an uncertainty in both the U (east) and V (north) components are also calculated as described in [8].

In this study, these uncertainties in the total combined vectors were found to decrease, in general, with the addition of elliptical data in the combining process. Uncertainties in the U and V directions both decreased on the order of 0 - 5 cm/s with the original uncertainty values in both directions being mostly between 0 -20 cm/s.

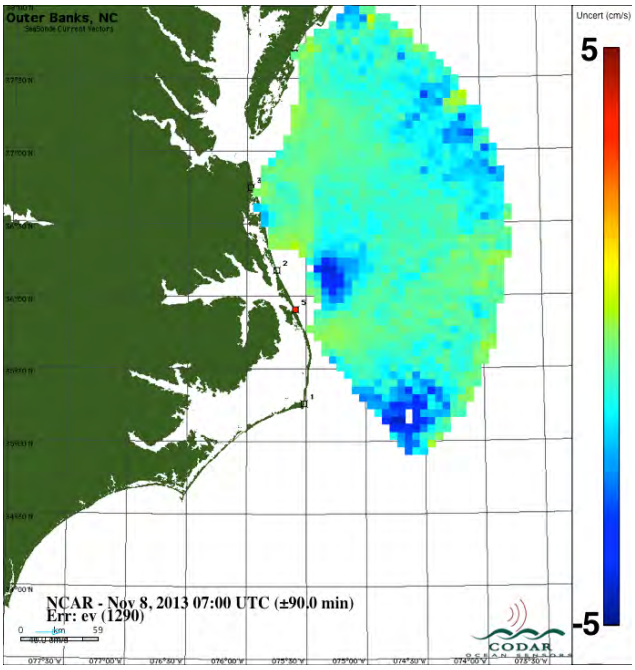

Fig. 5.: Map of mean difference in V uncertainties (cm/s) by adding elliptical vectors

Figures 4 - 7 were generated from 228,481 data points over the data collection period. The decreases in uncertainties were not spread uniformly across the field of measurements as shown in Figures 4 & 5. Areas of blue experienced the greatest decrease in uncertainties, potentially due to more noise in the radial measurements in that are. By adding more data sources, the statistical robustness increases, especially in areas of less certain monostatic data.

Histograms for various changes in uncertainties with the addition of elliptical data for U & V are shown in Figures 6 & 7, respectively. These include all grid points over the entire field of measurement for the entire time period of the study.

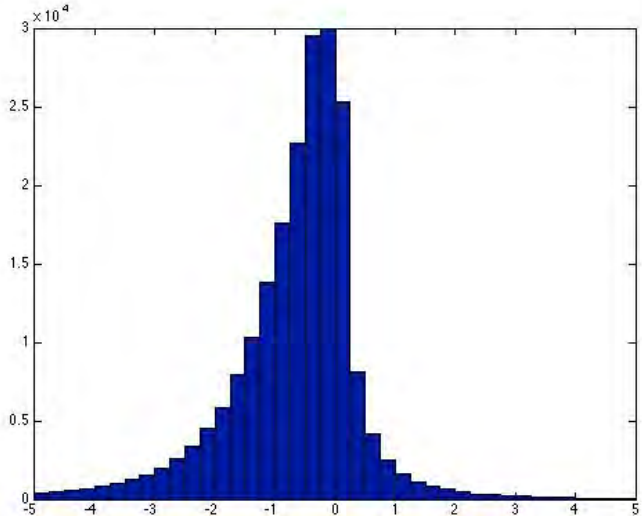

Fig. 6. Histogram of changes in the uncertainties for U component from radials-only processing and processing with both radial and elliptical vectors

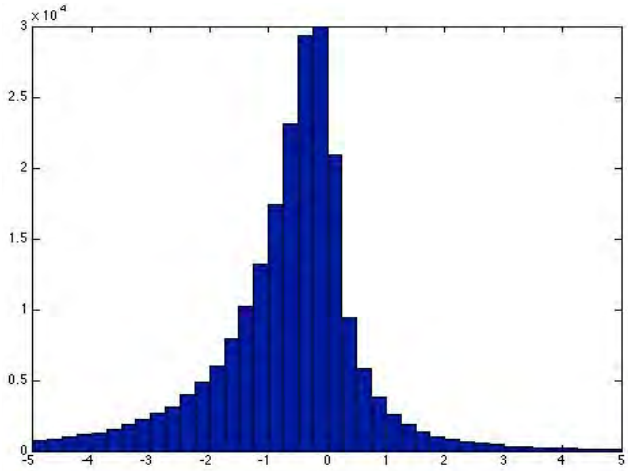

Fig. 7. Histogram of changes in the uncertainties for V component from radials-only processing and processing with both radial and elliptical vectors

III. Malta Channel Network

A. Network Description

While the multi-static configuration of the linear-arranged MARACOOS SeaSondes discussed above did not produce any increase in offshore range, multi-static operation can, under certain circumstances, provide additional spatial coverage of surface currents than might otherwise not be possible with only a mono-static configuration. The Malta Channel HFR network is split between two countries with systems on opposite sides of the channel.

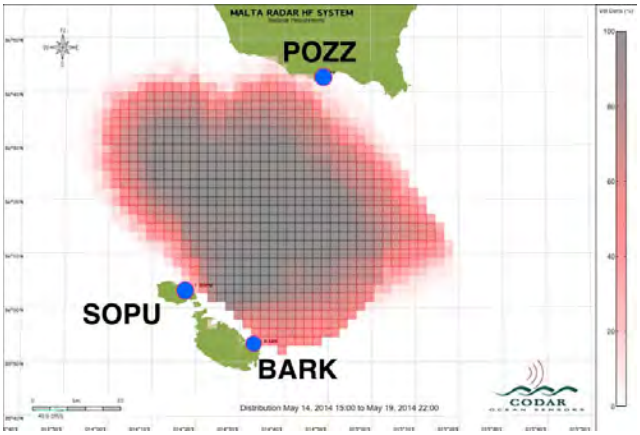

Fig. 8. Percent coverage of 2-D total vectors processed with radial vectors only.

A s shown in Figure 8, three SeaSonde stations are located at Ta' Sopu on Gozo (SOPU), Ta' Barkat on Malta (BARK) and Pozzallo Harbour on Sicily (POZZ). SOPU and BARK sites are owned and operated by the IOI-Malta Operational Centre of the University of Malta and POZZ site is the responsibility of the University of Palermo.

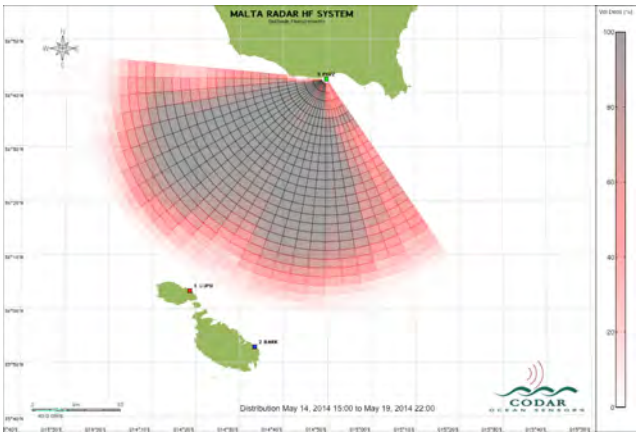

Fig. 9. Percent coverage of POZZ radial vectors

The radars in this network transmitted at 13.5 MHz during the ~5.5 day study period and were configured to share frequency using SHARE and collect multi-static data. Typical ranges for mono-static radial vectors were 60 – 75 km. Sweep offset timings were configured such that following bi-static pairs were created:

- POPU (POZZ receives sea echo from SOPU transmit)
- ELP1 (BARK receives sea echo from SOPU transmit)
- PORK (POZZ receives sea echo from BARK transmit)

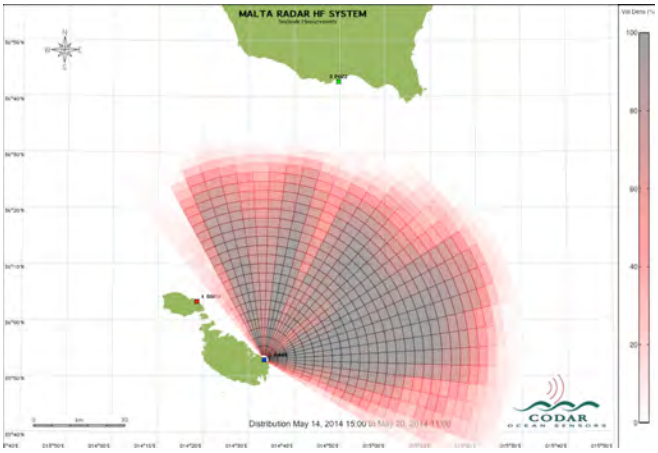

Fig .10. Percent coverage of BARK radial vectors

The triangular geometry of the Malta network with systems on opposite sides of the channel provides a different geometry than the MARACOOS network example. The reason for the limited coverage area when combing radial data only can be found in the radial vector percent coverage plots of the POZZ and BARK sites in Figures 9 & 10.

The distance across the channel is larger than the range of radial vector measurements. The total vector coverage to the southeast is limited by the lack of radial vectors from POZZ and the narrow crossing angle between the SOPU and BARK sites. By adding the PORK elliptical coverage area as shown in Figure 11, a significant increase in 2-D total vector coverage can be acheived by combining PORK (elliptical) and BARK (radial) data.

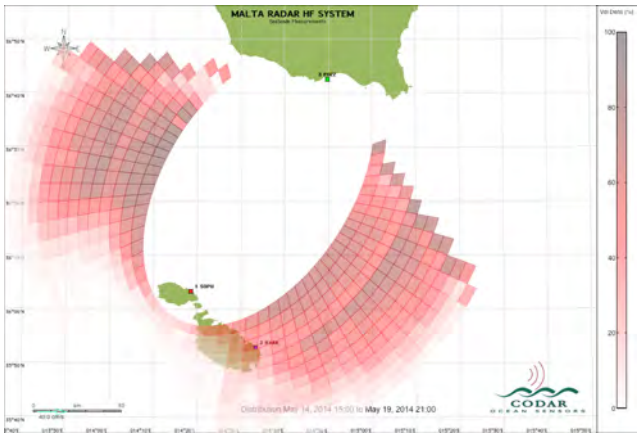

Fig. 11. Percent coverage of POPU elliptical vectors

The primary reason for the increased range of the PORK elliptical vectors to the Southeast is the shorter path for the radar transmission to travel from BARK to the scattering patch on the ocean surface back to the POZZ site. The POZZ mono-static transmission must travel out and back resulting in the path being exactly twice the range. The bi-static transmission must only cross the channel in one direction. For the five and a half day study period the spatial coverage of the total vector count increased approximately 41% after adding elliptical to the combining process with the gained areas primarily in the Southeast and Northwest. Figure 12 shows the resulting increased coverage area along with the original radials-only coverage outlined in blue.

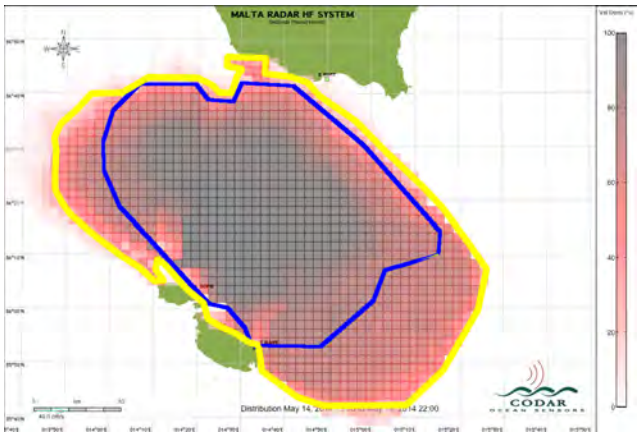

Fig. 12. Map of percent coverage of total vectors processed with radial vectors and elliptical vectors with edge of coverage outlined in yellow. Radials-only coverage is outlined in blue

IV. Conclusions

The two data sets examined here show that the addition of elliptical vectors in total vector creation can be beneficial to HFR networks in different ways. The data from the MARACOOS network shows a decrease in uncertainty values along with an increase in temporal coverage for grid points less

than the radials-only maximum range. The Malta data provides an example of a network configuration in which an increase in total vectors coverage area can be achieved. The benefits of adding multi-static operation to an HFR network depends on the site and coastline configurations. As more multi-static HFR networks are designed and deployed worldwide, the benefits of adding multi-static operation to these networks should be considered.

ACKNOWLEDGMENT

The authors would like to thank the following people for contributing their data and efforts for this study: Hans Widmer at Johns Hopkins University Applied Physics Lab, Mike Muglia at the University of North Carolina Coastal Studies Institute, Teresa Garner at Old Dominion University, Prof. Aldo Drago at the IOI-Malta Operational Centre of the University of Malta, Dr. Giuseppe Ciraolo at Università degli Studi di Palermo, and QualitasRemos.

REFERENCES

[1] Harlan, J., Terrill, E., Hazard, L., Keen, C., Barrick, D., Whelan, C., Howden, S., Kohut, J. "The integrated ocean observing system high-frequency radar network: status and local, regional, and national applications." *Mar. Technol. Soc. J.,* 2010*,* 44, 122–132.

[2] Fujii, S ML Heron, K Kim, JW Lai, SH Lee, X Wu, X Wu & LR Wyatt , 2013. An overview of developments and applications of oceanographic radar networks in Asia and Oceania countries, Ocean Science Journal, 48(1), 69-97.

[3] Teague, C.C., "Bistatic Radar Techniques for Observing Long Wavelength Directional Ocean- Wave Spectra," IEEE Trans., Geoscience Electronics, Vol.. 9, 211-215, (1971).

[4] Barrick, D.E., Remote Sensing of Sea State by Radar, Chapter 12 of Remote Sensing of the Troposphere, V.E. Derr, Editor, NOAA/Environmental Research Laboratories, Boulder, CO, 12.1-12.6." (1972).

[5] Barrick, D.E.; Lilleboe, P.M.; Lipa, B.J.; Isaacson, J. Ocean surface current mapping with bistatic HF radar. U.S. Patent 6,774,837, 2004.

[6] Barrick, D.E.; Lilleboe, P.M.; Teague, C.C. Multi-station HF FMCW radar frequency sharing with GPS time modulation multiplexing. U.S. Patent 6,856,276, 2001.

[7] Lipa, B.; Whelan, C.; Rector, B.; Nyden, B., "HF Radar Bistatic Measurement of Surface Current Velocities: Drifter Comparisons and Radar Consistency Checks," *Remote Sens.* 2009, *1*, 1190-1211.

[8] Lipa, B., "Uncertainties in SeaSonde current velocities," Current Measurement Technology, 2003. Proceedings of the IEEE/OES Seventh Working Conference, pp.95-100, 13-15 March 2003

[9] Kohut, J.T.; Glenn, S.M.; Roarty, H.J., "Recent results from a nested multi-static HF radar network for the NorthEast Observing System (NEOS)," OCEANS 2003. Proceedings , vol.4, no., pp.2335 Vol.4,, 22-26 Sept. 2003

[10] Kohut, J.T.; Glenn, S.M.; Roarty, H.J.; Schofield, O.M., "A Nested Multi-static HF Radar Testbed for the New York Bight and Beyond," OCEANS 2007 - Europe , vol., no., pp.1,3, 18-21 June 2007

[11] Roarty, H.; Kerfoot, J.; Kohut, J.; Glenn, S.; Whelan, C.; Hubbard, M., "Improving the measurements of high frequency radar: Reduced averaging times and bistatics," OCEANS - Bergen, 2013 MTS/IEEE , vol., no., pp.1,6, 10-14 June 2013